

Palaeoproterozoic structural evolution of polyphase migmatites in Olkiluoto, SW Finland



JON ENGSTRÖM^{1,2*}, AULIS KÄRKI³, SEPPO PAULAMÄKI⁴ AND IRMELI MÄNTTÄRI⁵

¹*Geological Survey of Finland, P.O. Box 96, FI-02151 Espoo, Finland*

²*Åbo Akademi University, FI-20500 Turku, Finland*

³*Kivitiето Oy, Teknologiantie 1, FI-90590 Oulu, Finland*

⁴*Gräsantörmä 11 B 24, FI-02200 Espoo, Finland*

⁵*Klariksentie 1 B 27, FI-02250 Espoo, Finland*

Abstract

In migmatitic environments the behaviour of the system is controlled by the generation and amount of the anatectic melt. Accordingly, migmatites typically show a genetic linkage between the tectonic deformation and melt migration. We investigated this relationship in Olkiluoto (SW Finland) and identified four phases of ductile deformation, which are distinguished by the multiple folding phases, ductile shear events and cross-cutting features associated with pegmatitic leucosomes and/or a specific type of diatexitic migmatite with feldspar megacrysts. U–Pb LA-MC-ICPMS data on zircon cores and rims from migmatites and cross-cutting pegmatites indicate two distinct metamorphic events associated with melt generation and migration at 1.87–1.84 Ga and 1.82–1.78 Ga. These two migmatitic events suggest that the orogenic evolution of the area was long-lasting and characterized by slow cooling. The structural data and the age constraints presented in this paper support the idea of similar tectonic evolution and metamorphic environment in SW Finland and central E Sweden.

Keywords: High-grade, migmatite, ductile deformation, shear structure, Olkiluoto site, SW Finland, slow-cooling orogen.

* Corresponding author (e-mail: jon.engstrom@gtk.fi)

Editorial handling: Arto Luttinen (e-mail: arto.luttinen@helsinki.fi)

1. Introduction

Migmatite belts are most typically associated with collisional orogenies, but migmatites may also form due to heating of the lower crust by underplating of subduction-related basaltic melts (Castro et al., 1999; Hegner et al., 2001; Stephens & Andersson, 2015; Stephens, 2020a). A genetic relationship between migmatites and granites has been documented from several orogens (Sawyer, 1998; Milord, 2001; Solar & Brown, 2001; Johannes et al., 2003), and spatial as well as temporal associations of granites with crustal-scale shear zones are common (Brown and Solar, 1998a, 1998b). The generation of migmatites is closely associated with the tectonic evolution and development of meso- and macroscopic geological structures of the bedrock. In a high-grade migmatitic environment, ductile structures and associated leucosomes are the key elements, and often the sole structures, in interpretation of the structural evolution of the area.

The central Fennoscandian shield comprises two major crustal domains of different age: the Archean province in the NE and the Svecofennian province in the SW (e.g. Gaál & Gorbatshev, 1987; Kohonen et al., 2021). The provinces are separated by a collisional boundary (Raahe-Ladoga cryptic suture; see Fig. 1). The Palaeoproterozoic bedrock in southern Finland consists to a large extent of granitoids and migmatites (Nironen, 2017). Based on lithological, geochemical and geochronological data, the Svecofennian crustal domain has been in Finland divided into two major lithotectonic units: 1) the Western Finland subprovince (WFS) and 2) the Southern Finland subprovince (SFS) (Fig. 1; Korsman et al., 1997; Väisänen et al., 2002; Lahtinen et al., 2005; Nironen, 2017). The Ljusdal lithotectonic unit in Central E Sweden (Högdahl & Bergman, 2020) is separated by the Gulf of Bothnia from southern Finland, and shows similar characteristics to the rocks and structures in SW Finland (Fig. 1). These similar features are comparable in magmatic activity and structural evolution coupled with the same style and timing of metamorphism (Kähkönen, 2005; Nironen,

2005; Bergman et al., 2008; Väisänen et al., 2012; Högdahl & Bergman, 2020).

This study focuses on resolving the complex interplay between migmatite formation and ductile structural geological history of the Olkiluoto study area. The Olkiluoto site is the location for the Finnish deep geological repository for spent nuclear fuel and this study is a part of the geological site characterisation. Our investigation provides new insights into the tectonic history of the Olkiluoto site and SW Finland during the Palaeoproterozoic Svecofennian orogeny. The relationship between ductile deformation structures and migmatite formation in crystalline Palaeoproterozoic bedrock has not previously been studied in detail in this area. Even though the Olkiluoto investigation area is small, the results of this study can be connected to a more regional context regarding the tectonic framework in southern Finland.

2. Geological setting of the study area

2.1. Tectonic framework

The Palaeoproterozoic Svecofennian orogeny (in Sweden ‘Svecokarelian orogeny’; see Stephens, 2020b), and the corresponding crustal province (Fig. 1), have been conceptually well-established since the classic review of Gaál & Gorbatshev (1987). Several tectonic evolution models has been presented for the evolution of the accretionary orogen (Gaál & Gorbatshev, 1987; Lahtinen, 1994; Korsman et al., 1999; Lahtinen et al., 2005). The orogeny commenced with a main collisional stage between 1.92 Ga and 1.87 Ga (Nironen, 2017 and references therein), in which several volcanic arc complexes or microcontinents laterally accreted into the margin of the Archean Karelia craton (e.g. Lahtinen et al., 2005). During this convergence, several thrust sheets developed within a W–SW to E–NE compressional environment in southern Finland (Nironen, 2017; Torvela &

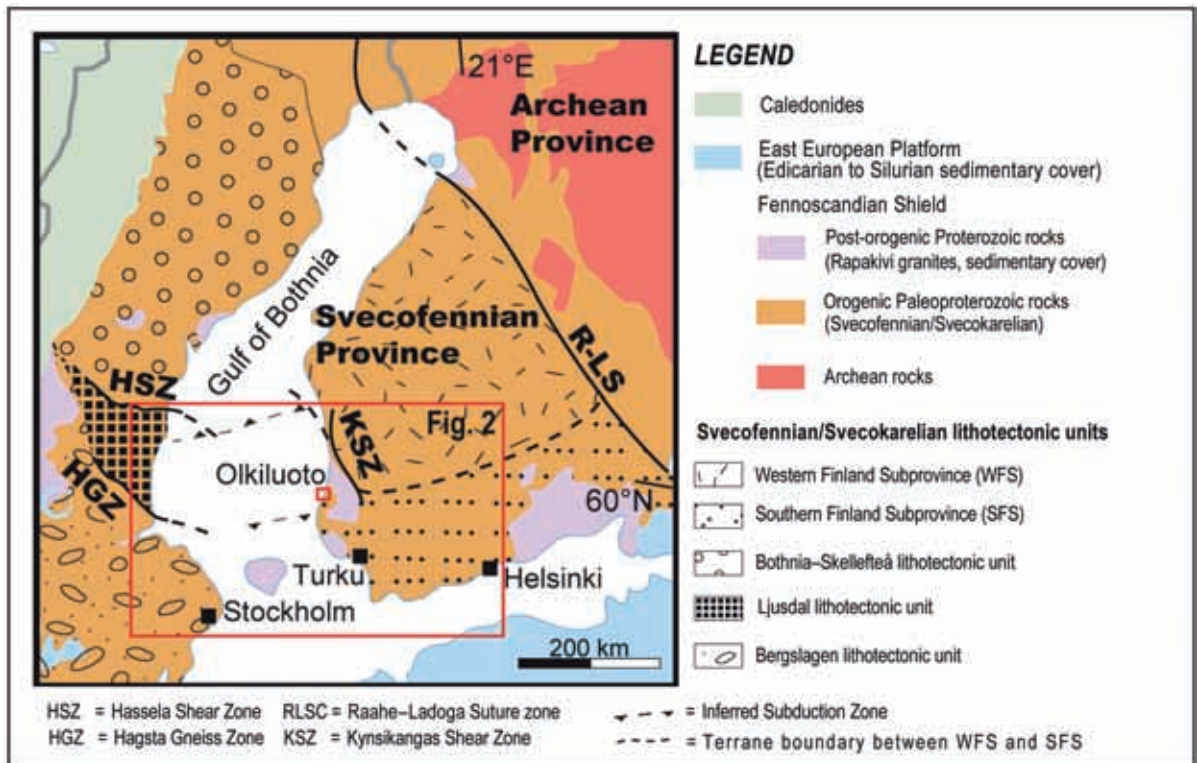


Figure 1. Geological map of the Fennoscandian shield. Olkiluoto is indicated with a red square. Map modified from Koistinen et al., 2001; Korja & Heikkinen, 2005; Nironen, 2017; Stephens, 2020a; Stephens, 2020b.

Kurhila, 2020). In the Western Finland subprovince (WFS) moderate crustal thickening resulted in the development of a widespread formation of granites and associated migmatites, exemplified in the Vaasa region (Mäkitie et al., 2012; Chopin et al., 2020). The next tectonic phases included minor crustal extension, followed by a final successive orogenic convergence that resumed at ca. 1.84 Ga (Lahtinen et al., 2005; Torvela et al., 2008; Torvela & Kurhila, 2020). This transpressional deformation phase initiated intensive folding and shear zone development in southern Finland (Väisänen et al., 2002; Väisänen & Skyttä, 2007; Torvela & Kurhila, 2020).

The two main metamorphic events during the Svecofennian orogeny are of the high-T/low-P type. The early Svecofennian metamorphism at 1.88–1.87 Ga generally reached upper amphibolite facies, and can be detected throughout the

Finnish Svecofennian (Korsman et al., 1999; Nironen, 2017). The late Svecofennian high-T metamorphism at 1.84–1.80 Ga reached granulite facies in large areas of southernmost Finland and was associated with emplacement of granites together with anatexis resulting in formation of migmatites and pegmatites during the late stages of the Svecofennian orogeny (Huhma, 1986; Korsman et al., 1999; Väisänen & Hölttä, 1999; Väisänen et al., 2002; Skyttä & Mänttari, 2008).

In central E Sweden, the Ljusdal lithotectonic unit (Högdahl & Bergman, 2020) (see Figs. 1, 2) is bounded on three sides by complex systems of ductile shear zones. In the Gulf of Bothnia, towards Finland in the E, the lithotectonic boundaries are concealed by the Mesoproterozoic to Early Palaeozoic sedimentary cover (Högdahl & Bergman, 2020; Wickström & Stephens, 2020). Two of the

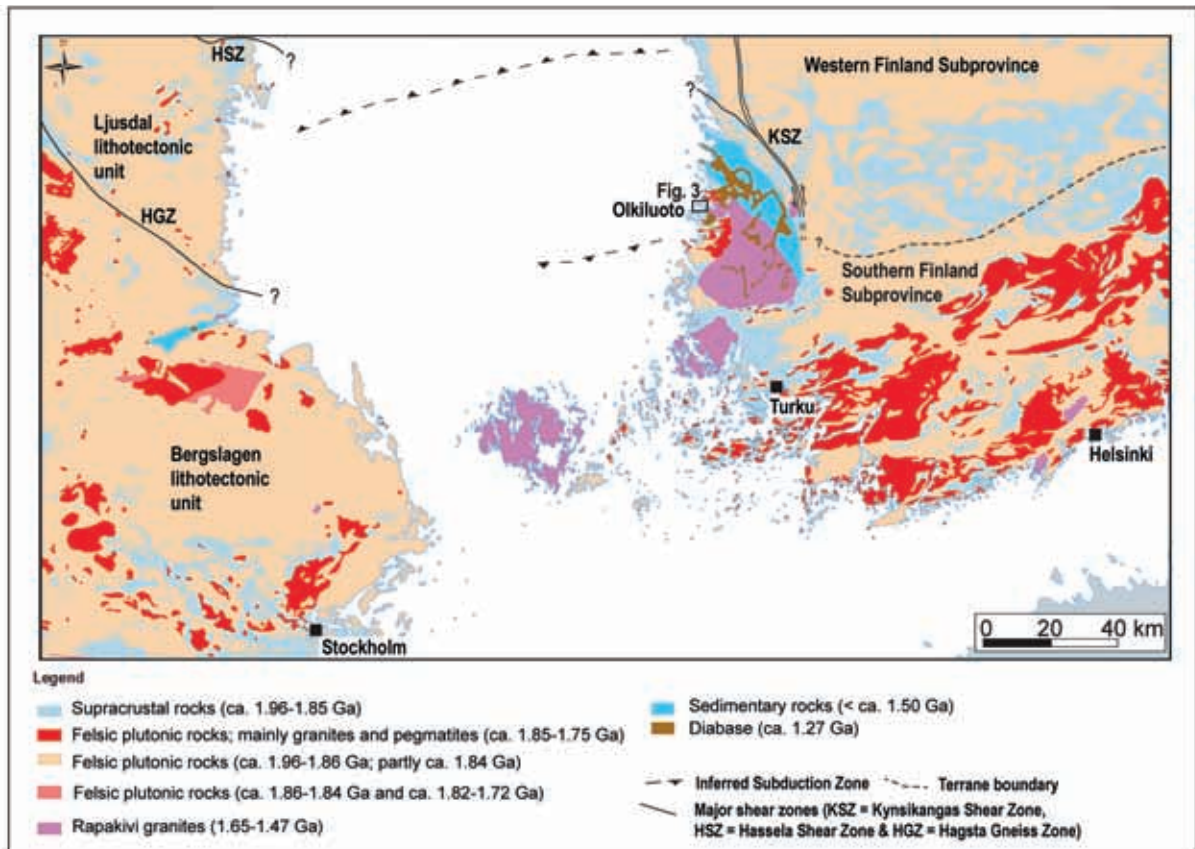


Figure 2. Geological map of SW Finland and central-E Sweden modified from Koistinen et al., 2001; Korja & Heikkinen, 2005; Nironen, 2017; Högdahl & Bergman, 2020.

major ductile shear zones (Hassela Shear Zone & Hagsta Gneiss Zone) separate the Ljusdal lithotectonic unit from lithotectonic units to the N (Botnia-Skellefteå) and S (Bergslagen) (Fig. 1). The rocks within the Ljusdal lithotectonic unit were affected by polyphase, ductile deformation and two episodes of high-grade, low-pressure metamorphism during the Svecofennian orogeny (Högdahl et al., 2008; Högdahl & Bergman, 2020).

The BABEL seismic profiles recorded in the Bothnian Basin in between Sweden and Finland provide insights into the possible connections between the major geological units (Korja et al., 2001; Korja & Heikkinen, 2005; Buntin et al., 2019). The BABEL interpretation by Korja & Heikkinen (2005) suggests crustal stacking from a SW direction and implies a subduction zone further

south. From the BABEL profiles, it is also possible to distinguish a NE-dipping crustal structure that underlies the Bothnian Basin (BABEL Working Group, 1993; Korja & Heikkinen, 2005). Korja & Heikkinen (2005) inferred that these crustal features are collisional structures that record the last stages of the convergence between two colliding microplates. They interpreted the mantle reflection to host remnants of a NE-dipping Palaeoproterozoic subduction zone (Fig. 2) prior to the main collisional event (1.89–1.87 Ga). Based on the seismic interpretations, an extensional event between the first main collisional stage and the next accretionary stage (1.84–1.81 Ga) has been suggested (Korja & Heikkinen, 2005; Högdahl & Bergman, 2020).

migmatites, and leucosome production took place in several stages under high- T conditions in the Palaeoproterozoic crust. There are indications of two different metamorphic events in Olkiluoto (Tuisku & Kärki, 2010). The metamorphic peak of the first event is estimated to have taken place at a pressure of approximately 6 kbar and is indicated by leucosome development at an early stage of the ductile deformation (Tuisku & Kärki, 2010). The mineral assemblages of the second metamorphic peak are indicative of upper amphibolite facies. Pressure and temperature conditions during the culmination of this metamorphic event, calculated and predicted from mineral assemblages, were 660–700 °C and 3.5–4.0 kbar (Tuisku & Kärki, 2010).

3. Methods of the study

3.1. Structural geological mapping and U–Pb zircon dating samples

During the site characterisation work in Olkiluoto, the structural geology and the metamorphic features have been investigated. The study focused on delineating the ductile structural geological evolution at the Olkiluoto site by comparing the results of detailed geological structural mapping and the results of targeted age determinations. Detailed geological mapping of surface outcrops, underground observation in ONKALO® (the access tunnel of the high-level nuclear waste repository) and the deep drill hole information have been coupled into a geological site model. In the present study, the main method was detailed structural observation of the cleaned surface outcrops. The structural analysis included mapping of features such as fabric and fold orientation, cross-cutting relationships, and kinematic indicators. At selected locations, sawed samples were utilized to outline the structures in 3D. Even though the main focus was on the meso- and macro-scale structures, a few thin sections were prepared to examine the structures at the micro-scale.

To link the metamorphic migmatitic environment to the structural model, two observation and sampling sites were selected in the underground research facility (ONKALO®), where the cross-cutting relationship between older migmatite bedrock and younger pegmatitic leucosome could be defined. In order to constrain the age relationship between the different phases of ductile deformation, four samples from two sampling sites were obtained within the ONKALO® tunnel. The samples represent two different cross-cutting pegmatitic dykes and the adjacent leucosomes in the nearby migmatites. The samples A2019 and A2021 were collected from D_1 leucosomes in the proximity of the pegmatitic samples A2018 and A2020. Sample A2018 was taken from a ca. 0.5-m-wide pegmatitic leucosome vein, occurring parallel to the S_3 axial surfaces. Sample A2020 was collected from a N–S-striking, moderately E dipping, 3–5 m wide pegmatitic leucosome dyke.

3.2. U–Pb zircon dating with LA-MC-ICP-MS

Zircon grains for LA-MC-ICPMS (*laser ablation multicollector inductively coupled plasma mass spectrometry*) U–Pb dating were selected by hand-picking after heavy liquid and Frantz magnetic separation. The chosen grains were mounted in epoxy resin and sectioned approximately in half and polished. Back-scattered electron images (BSE) and cathodoluminescence (CL) images were taken using a scanning electron microscope (SEM) to target the spot analysis sites on mineral grains.

U–Pb dating was performed using a Nu Plasma HR multicollector ICPMS at the Geological Survey of Finland in Espoo using a technique very similar to that of Rosa et al. (2009), except that a New Wave UP193 Nd YAG laser microprobe was used. Samples were ablated in He gas (gas flow = 1.0 l/min) using a low volume teardrop-shaped (<2.5 cm³) laser ablation cell (Horstwood et al., 2003). The He aerosol (gas flow = 0.3 l/min) was

mixed with Ar (gas flow = 1.1 l/min) in a Teflon mixing cell prior to entry into the plasma. The gas mixture was optimized daily for maximum sensitivity and all analyses were conducted in static ablation mode. The ablation conditions were: beam diameter 20–35 μm , pulse frequency 10 Hz and beam energy density 1 J/cm². A single U–Pb measurement included 30 s of on-mass background measurement, followed by 90 s of ablation with a stationary beam. Masses 204, 206 and 207 were measured in secondary electron multipliers and 238 in the extra high mass Faraday collector. Ion counts were converted and reported as volts by the Nu Plasma time-resolved analysis software. ²³⁵U was calculated from the signal at mass 238 using a natural ²³⁸U/²³⁵U = 137.88. Mass number 204 was used as a monitor for common ²⁰⁴Pb. Raw data were corrected for background, laser-induced elemental fractionation, mass discrimination and drift in ion counter gains, and they were reduced to U–Pb isotope ratios by calibration to concordant reference zircon of known age, using protocols adapted from Andersen et al. (2004) and Jackson et al. (2004). Standard zircon GJ-01 (609 \pm 1 Ma; Belousova et al., 2006) and an in-house standard zircon A382 (1877 \pm 2 Ma; Huhma et al., 2012) were used for calibration. Age-related common lead (Stacey & Kramers, 1975) correction was used when the analysis showed common lead contents above the detection limit. The calculations were performed off-line using an interactive spreadsheet program written in Microsoft Excel/ VBA by Tom Andersen (Rosa et al., 2009). To compensate for drift in instrument sensitivity and Faraday vs. electron multiplier gain during an analytical session, a correlation of signal vs. time was assumed for the reference zircons. A description of the algorithms used is provided in Rosa et al. (2009).

Plotting of the U–Pb isotopic data and the age calculations were performed using the Isoplot/Ex 3 program (Ludwig, 2003). All the ages were calculated with 2 σ errors and without decay constants errors. Data-point error ellipses in the figures are at the 2 σ level.

4. Ductile deformation and structural sequence in Olkiluoto migmatites

In the following, we present evident overprinting relationships between the observed deformation structures. Four separate deformation phases have been determined and at least two migmatization events have been identified. Thus, the evolution of ductile deformation can be determined, and subsequent deformation processes are possible to establish.

4.1. Primary sedimentary structures and D₁ deformation

Primary bedding (S_0) is rarely preserved, but it can be observed as refractory lithologies in boudin chains or layers. In places, the lithological layering, plausibly reflecting originally pelitic and psammitic beds in a turbidite sequence, can be inferred from the different degrees of partial melting. The pelitic (mica-rich) parts are migmatized, whereas the psammitic parts are better preserved.

At a few locations, this compositional layering was folded during the D₁ deformation phase, and some indication of leucosome growth is also observed (Fig. 4a). The first ductile deformation phase (D₁) pervasively affected the bedrock of the whole study area. The best evidence is found in the northern part of the island. In the metapelites, the first phase of strong migmatization is present as small leucosomes that are tightly folded, displaying rootless and intrafolial F₁ folds, as well as sheath-type fold structures (Fig. 4b, e). In the more competent TGG rock, the D₁ deformation is observed as S₁ metamorphic banding with an E–W orientation and a moderate to steep dip towards S (Fig. 4c, d, f). Another prominent indication of the first deformation phase is the observed lineation in the N part of Olkiluoto island, where the feldspar minerals are stretched and elongated in

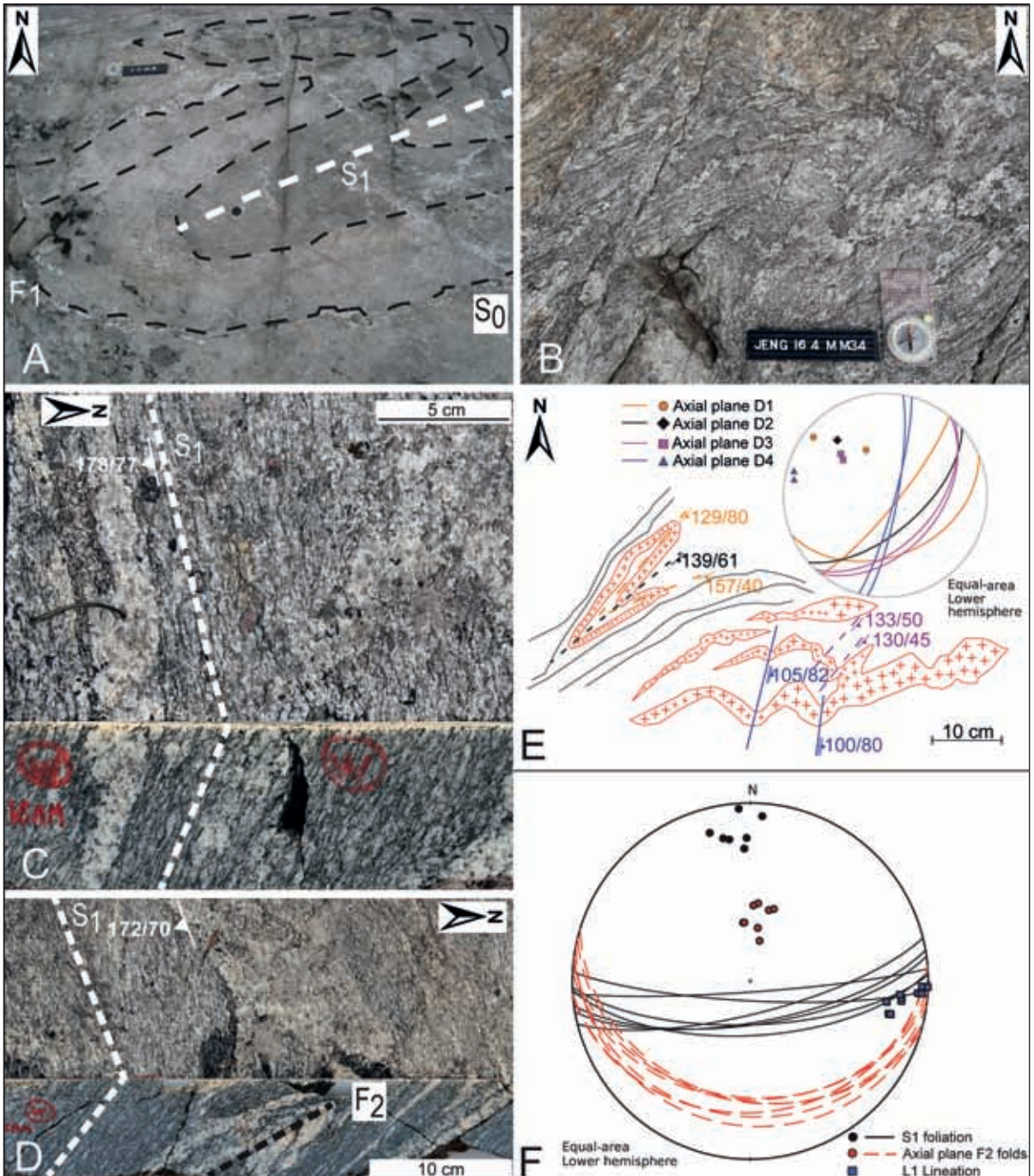


Figure 4. D₁ structures illustrated by photos, sketches and stereographic projections. The locations of outcrops are indicated in Figure 3. a) A close F₁ fold structure in a psammitic to pelitic metasedimentary rock. The primary bedding can be recognized by the variation of the mica content in different layers. b) Horizontal section of intensely folded leucosomes that display rootless and intrafolial F₁ folds (re-folded in D₂). c) Horizontal/vertical section of a TGG rock that displays metamorphic S₁ foliation. d) Horizontal/vertical section of TGG rock that displays S₁ foliation and F₂ folds with E-W-oriented axial planes with shallow dip towards S. e) Sketch illustrating the polyphase folded diatexitic migmatite shown in the photo above in 4b. f) Stereographic projection illustrating the E-W-oriented S₁ foliation, with a steep dip towards S. The S₂ axial planes shows a more shallow dip towards S and the lineation plunges shallow towards ESE.

an E–W orientation with a gentle plunge towards ESE (Fig. 4c, d). The lineation is mostly found in larger TGG rock bodies as stretching lineation L_1 , where the lineation has been formed parallel to the tectonic transport direction. (Fig. 4f).

4.2. D_2 deformation

D_2 ductile deformation has affected the bedrock of the whole island, generating tight folds of leucosome veins formed during D_1 . The main structural D_2 elements are tight to isoclinal F_2 folds with sporadically observed axial surface foliation, with mainly mica growth. In the outcrops, the symmetrical, tight F_2 folds typically show

wavelengths of a few centimetres and amplitudes of a few decimetres. These, nearly isoclinal structures that are virtually impossible to detect on planar outcrop surfaces but are evident in vertical sections and underground (Fig. 5). The F_2 folds are present throughout the study area but are most obvious in the migmatitic rocks in the NW part of the island, where the later structural overprinting is not pervasive. In the NW part, the F_2 axial planes dip moderately gently to the S and the F_2 fold axes plunge gently or subhorizontally towards the E (Fig. 5). In places, the observed lineation in the migmatitic rock represents an intersection lineation between S_1 and S_2 , ($L_{1/2}$), plunging gently towards the E.

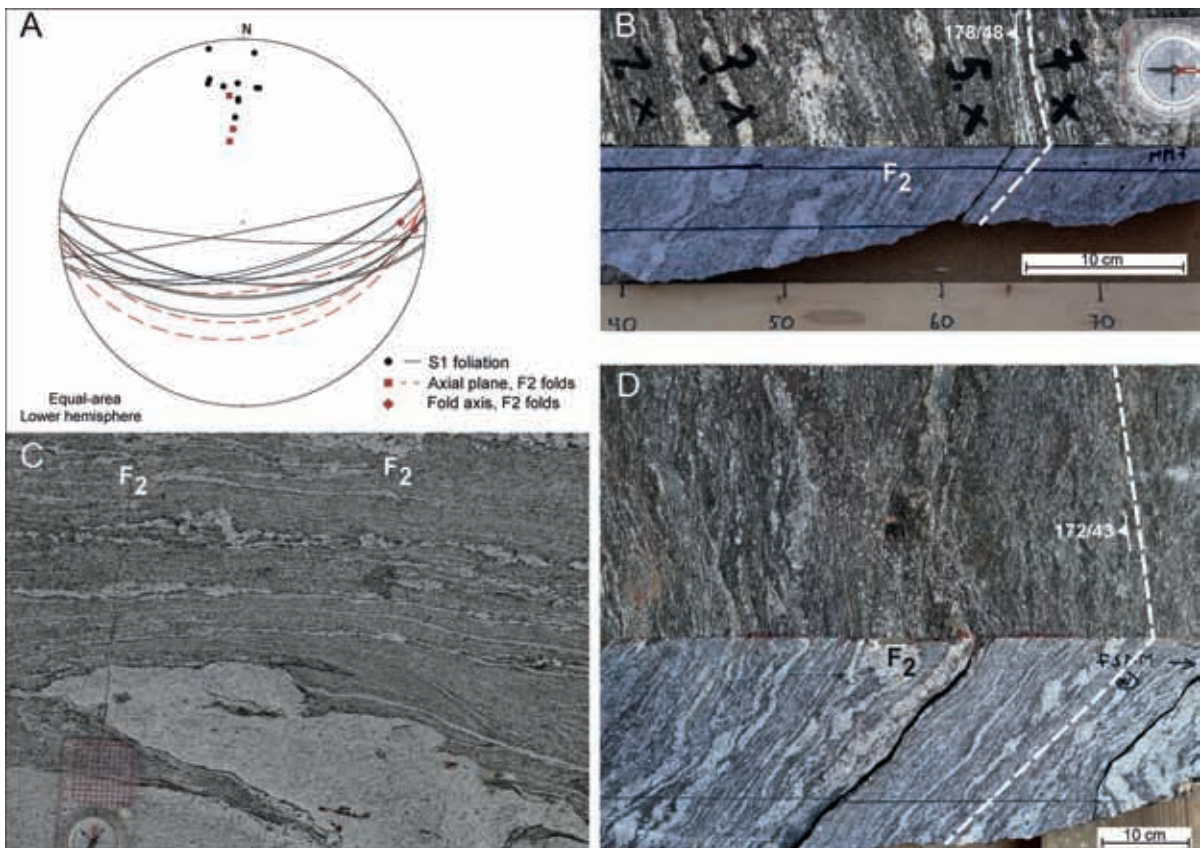


Figure 5. D_1 and D_2 deformation phases illustrated by photos, sketches and stereographic projections. The locations of outcrops are indicated in Figure 3. a) Stereographic projection illustrating S_1 foliation and F_2 folds with E–W-oriented axial planes and a dip towards S. b) Horizontal/vertical section of F_2 folds in a metatextitic migmatite, showing a tight appearance of F_2 folds. c) Horizontal section of F_2 folds in a metatextitic migmatite, with a typical isoclinal appearance. d) Horizontal/vertical section of F_2 folds in a metatextitic migmatite. The axial surface dips to the south and the fold axis is almost horizontally plunging towards the E.

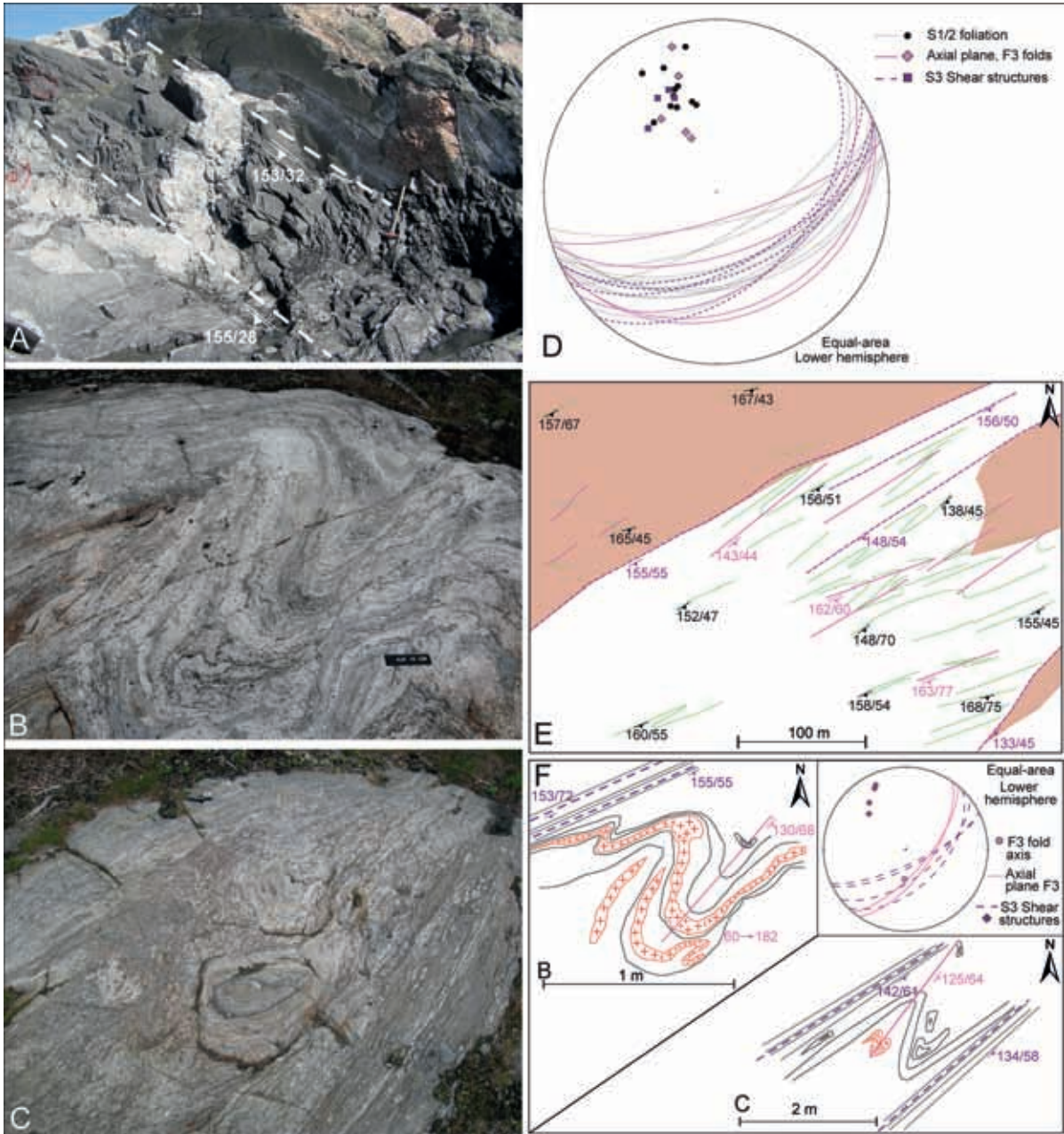


Figure 6. D₃ deformation phase illustrated by photos, sketches and stereographic projections. The locations of outcrops are indicated in Figure 3. a) Vertical section of open-close F₃ folds in a metatextitic migmatite, with axial planes dipping towards SE. b) Horizontal section of a close F₃ fold in diatextitic migmatite, with the F₃ axial plane dipping moderately towards SE. c) Horizontal section of close F₃ folds in diatextitic migmatite, with the development of shearing along fold limbs. d) Stereographic projection illustrating the structures with axial planes dipping SE and with D₃ shear structures orientated parallel to limbs of the F₃ folds. e) Map view illustrating the open to close F₃ folding, showing F₃ axial planes and D₃ shear structures. f) Stereographic projection and sketches with structures from outcrops B & C, with the F₃ axial plane trending NE-SW and the D₃ shear structures along limbs F₃ folds.

4.3. D_3 deformation

The third deformation phase (D_3) is characterised by F_3 folds and D_3 shear structures, and the impact of this process is localized. The folds are observed all over Olkiluoto, whereas the major D_3 strain has been partitioned into the E–W-striking shear zones especially in the northern and central parts of the island. In the fold interference patterns, the F_3 elements are identified as open-close folds deforming earlier stage leucosomes and planar structures. The axial planes of these folds usually dip towards the SE (Fig. 6a, d, e). However, S_3 axial plane foliation is only rarely developed. In the diatexitic migmatites, these folds typically show shear structures along the limbs, and these have occasionally evolved into wider shear zones (Fig. 6b, c, f). Especially in the central part of the island, wide granitic pegmatoid dykes (D_3 leucosomes) have migrated or developed parallel to the S_3 axial surfaces (Fig. 3). In the folded, layer-structured migmatites, short tears along axial surfaces are filled with new narrow pegmatitic to granitic leucosomes.

The most prominent E–W-striking D_3 shear structures are composed of high-grade fault rocks, which nearly obliterate all structures of earlier deformations (Fig. 7a, b, f). Individual shear bands or stacks can range from several millimetres to tens of centimetres. These shear bands are composed of pervasively foliated, coarse-grained fault rocks in which only mica minerals are clearly orientated. Evident kinematic indicators are not common within the shear bands. However, the lensoid objects are mostly symmetrical and, for example, detected as K-feldspar grain aggregates with fibrolitic sillimanite trails (Fig. 7c, d, e). Therefore, dextral rotation of axial surfaces of F_3 or earlier F_2 folds within the vicinity of these shear bands is the best kinematic indication for these shear zones (Fig. 7b). Locally, wider shear zone networks are composed of several stacks of distinct E–W-orientated shear bands. These networks have a total width that ranges from about one metre to tens of metres. Commonly, these networks have less deformed rock in between with small-scale folds

(Fig. 7b) and occasionally smaller interconnected step-over shear zones with a NE–SW orientation on the limbs of these folds.

4.4. D_4 deformation

All previous structures have been deformed by the meso- to macro-scale folds of the fourth phase of regional deformation (D_4). However, the strongest impact of this deformation is restricted to only a few subareas, and the most prominent D_4 structures are found in the central and eastern parts of Olkiluoto. The geometry of the F_4 folds varies from symmetric to asymmetric and from close to tight. Although most migmatization commenced during earlier deformation phases, a small amount of leucosome is associated with F_4 folds as narrow granitic veins parallel to the S_4 axial planes. The types and shapes of the final interference structures are strongly controlled by the rheological properties of the deformed lithologies. The simplest interference structures are composed of, for example, tight F_2 fold components that are refolded to close F_4 folds (Fig. 8b). The hinge lines of F_4 fold structures are well outlined, but the development of clear S_4 axial surface foliation is uncommon (Fig. 8a, b). The F_4 axial surfaces dip moderately or steeply towards the ESE, whereas the F_4 fold axis mostly plunges moderately towards the S (Fig. 8). The shapes of the F_4 folds have appearance of angular, box-type folds to chevron-type folds (Fig. 8a). The amplitude–wavelength ratios vary considerably and all variations, from tight, almost isoclinal to gentle folds, have been identified on outcrops and are also evident at the map pattern scale (Fig. 8d). The amplitudes of the most typical mesoscopic F_4 folds usually vary from tens of centimetres up to metres.

Shear bands are sparsely formed on the limbs of the F_4 folds (Fig. 9b), but NE–SW-striking shear zones in the surface section are the most prominent D_4 shear structures. They are several tens of centimetres to a few metres wide and are characteristically composed of a diatexitic migmatite type with roundish quartz-feldspar



Figure 7. D_3 deformation phase illustrated by photos, sketches and stereographic projections. The locations of outcrops are indicated in Figure 3. a) Horizontal section of an E-W-oriented shear zone within metatextitic migmatite. The intense shearing nearly obliterates all earlier structures. b) Close-up of the shear zone from photo 7a, illustrating rotated F_2 or F_3 folds with E-W-oriented shearing dipping towards S. Stereographic projection shows structures from the whole outcrop. c) Drillcore from the E-W-oriented shear zone showing clear grain size reduction. d) Thin-section image showing fibrolitic sillimanite growing parallel to foliation. Plane-polarised light. e) Thin-section image showing fibrolitic sillimanite growing at the edge of K-feldspar. Cross-polarised light. f) Vertical section of an E-W orientated shear zone within metatextitic migmatite from the ONKALO® research tunnel. The intense shearing nearly obliterates all earlier structures.

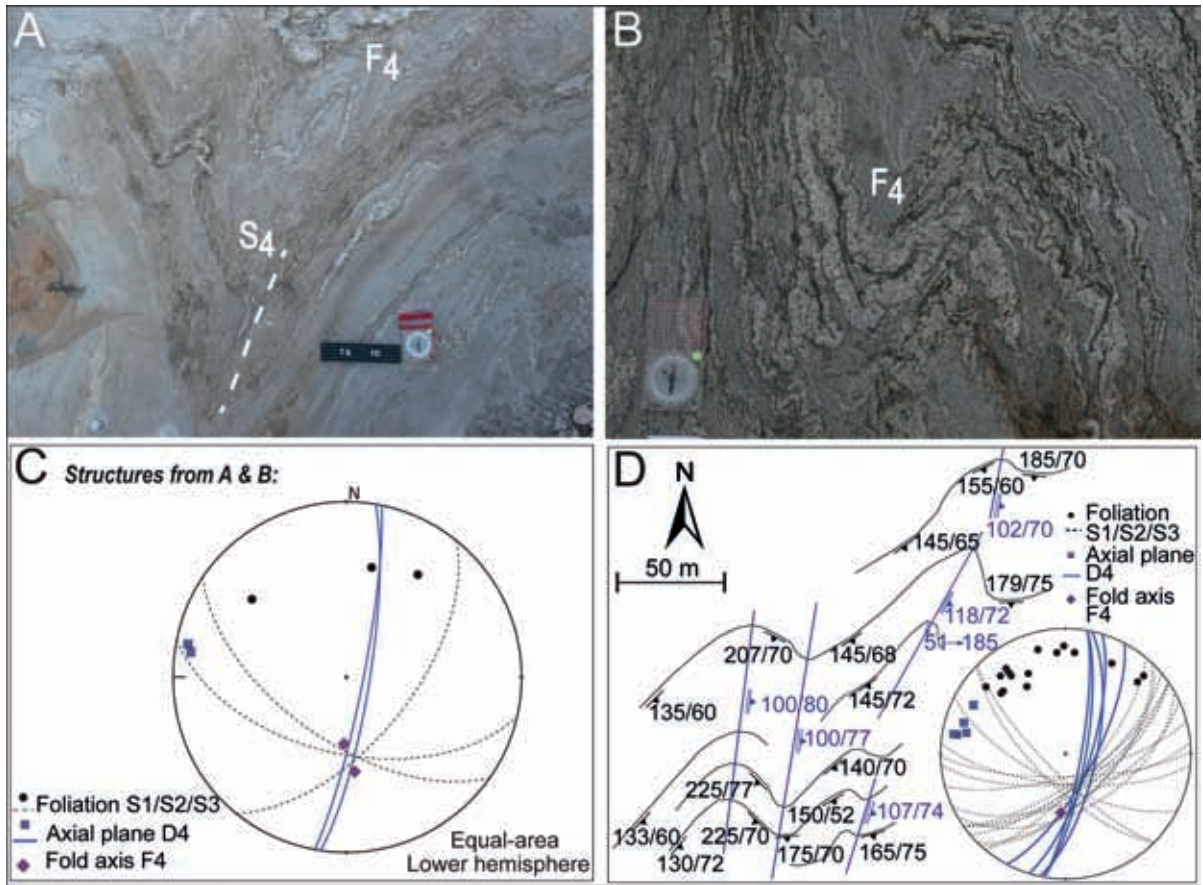


Figure 8. D_4 deformation phase illustrated by photos, sketches and stereographic projections. The locations of outcrops are indicated in Figure 3. a) Horizontal section of metatexitic migmatite illustrating an F_4 fold with the development of rarely seen axial plane S_4 foliation. b) Horizontal section of metatexitic migmatite illustrating re-folded F_2/F_3 folding during the D_4 deformation. c) Stereographic projection showing structures from both outcrops with the F_4 axial planes trending NNE-SSW and the F_4 fold axis plunging moderately towards S. d) Sketch showing meso-scale structures with folded $S_1/S_2/S_3$ foliation and the development of open F_4 folding. The stereographic projection shows axial planes trending NNE-SSW and the F_4 fold axis plunging moderately towards S.

aggregates or megacrysts, which overprint the older structures (Fig. 9a, c). The contact between the diatexitic migmatite with quartz-feldspar megacrysts and the country rock varies from gradational to sharp (Fig. 9c, d). This type of diatexitic migmatite has been observed in several places in the access tunnel of the underground research facility (ONKALO®), where they exhibit narrow, up to 2-metre-wide sub-horizontal units with varying orientation (Fig. 9d). The

main structural elements created by D_3 and D_4 deformations may closely resemble each other. However, the distinct diatexitic megacryst migmatite in D_4 implies a different environment during D_4 than D_3 , and this, combined with the differences in fold structures, indicates the occurrence of these two separate deformation phases.

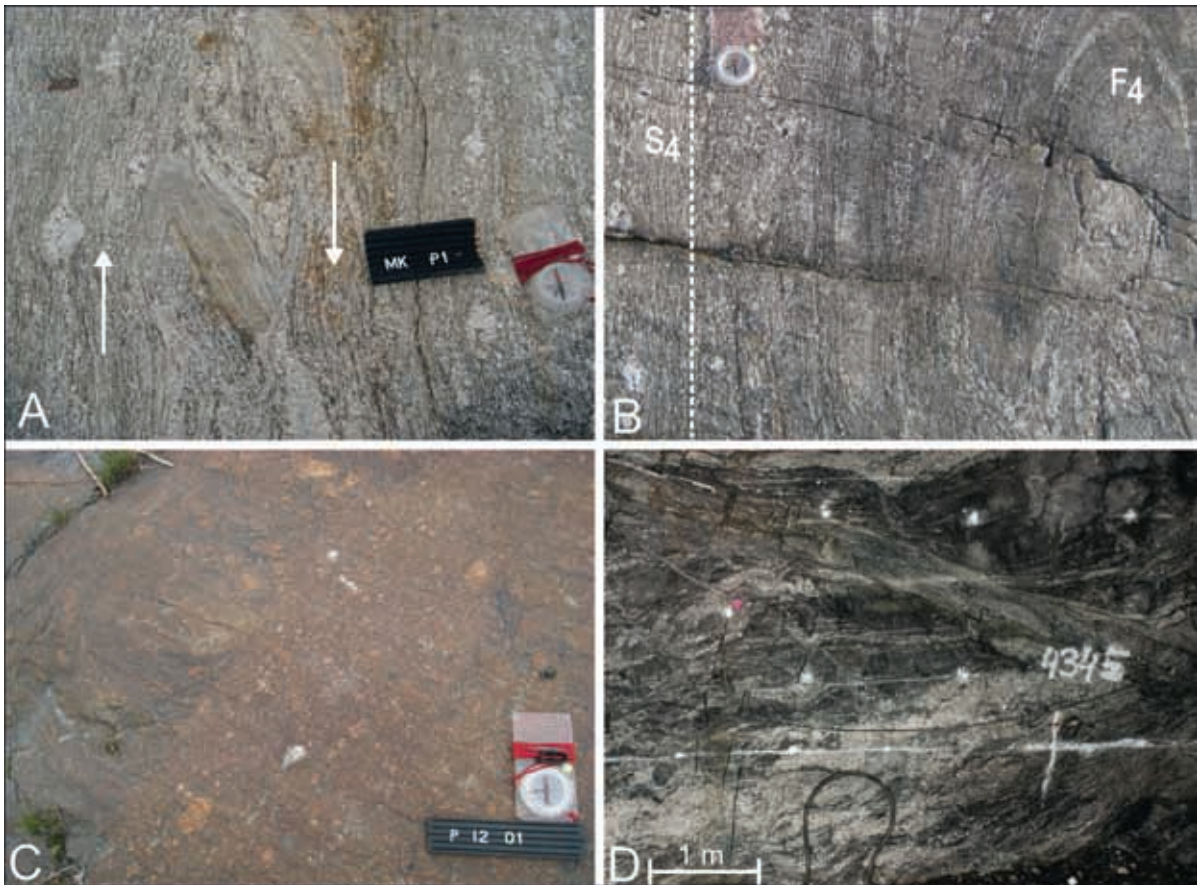


Figure 9. Photos of the D_4 deformation phase. The locations of outcrops are indicated in Figure 3. a) Horizontal section of NNE-SSW-oriented D_4 shear zone of the diatextitic migmatite type, with roundish quartz-feldspar aggregates or megacrysts that totally overprint older structures. b) AN-S-oriented D_4 shear zone on the limbs of an F_4 fold with a gradational contact to the diatextitic megacryst migmatite. c) Horizontal section of NE-SW-oriented D_4 shear zone with a sharp contact to the diatextitic megacryst migmatite. d) Vertical section of diatextitic megacryst migmatite observed in the ONKALO® research tunnel as narrow, ca. 1-m-wide sub-horizontal units. View towards S.

5. U–Pb Geochronology

5.1 Age Results

The migmatitic leucosome samples A2019 and A2021 were picked out from a homogenous part of the migmatitic rock, and thus as little as possibly unaffected structurally from later phases of deformation. Samples A2019 and A2021 were analysed and zircon U–Pb ages were calculated on the migmatite rock to define the metamorphic age of the rock. The more preserved cores of metamorphic zircon domains in A2019 and A2021 leucosomes yielded mean concordia ages of

1858±7 Ma and 1851±8 Ma, respectively (Fig. 10). This indicates that the age of the migmatite samples is determined at ca. 1.87–1.84 Ga, being contemporaneous with the formation of TGG gneisses from the Olkiluoto area (Mänttari et al., 2006; Mänttari et al., 2007). The more preserved zircon grain cores and their concordia age is interpreted to reflect the leucosomes for the first migmatite event (Fig. 10). The weakly zoned grains are defined to reflect some overgrowth from later phases of deformation, while the inherited grains reflect older Archean ages and are omitted from this study.

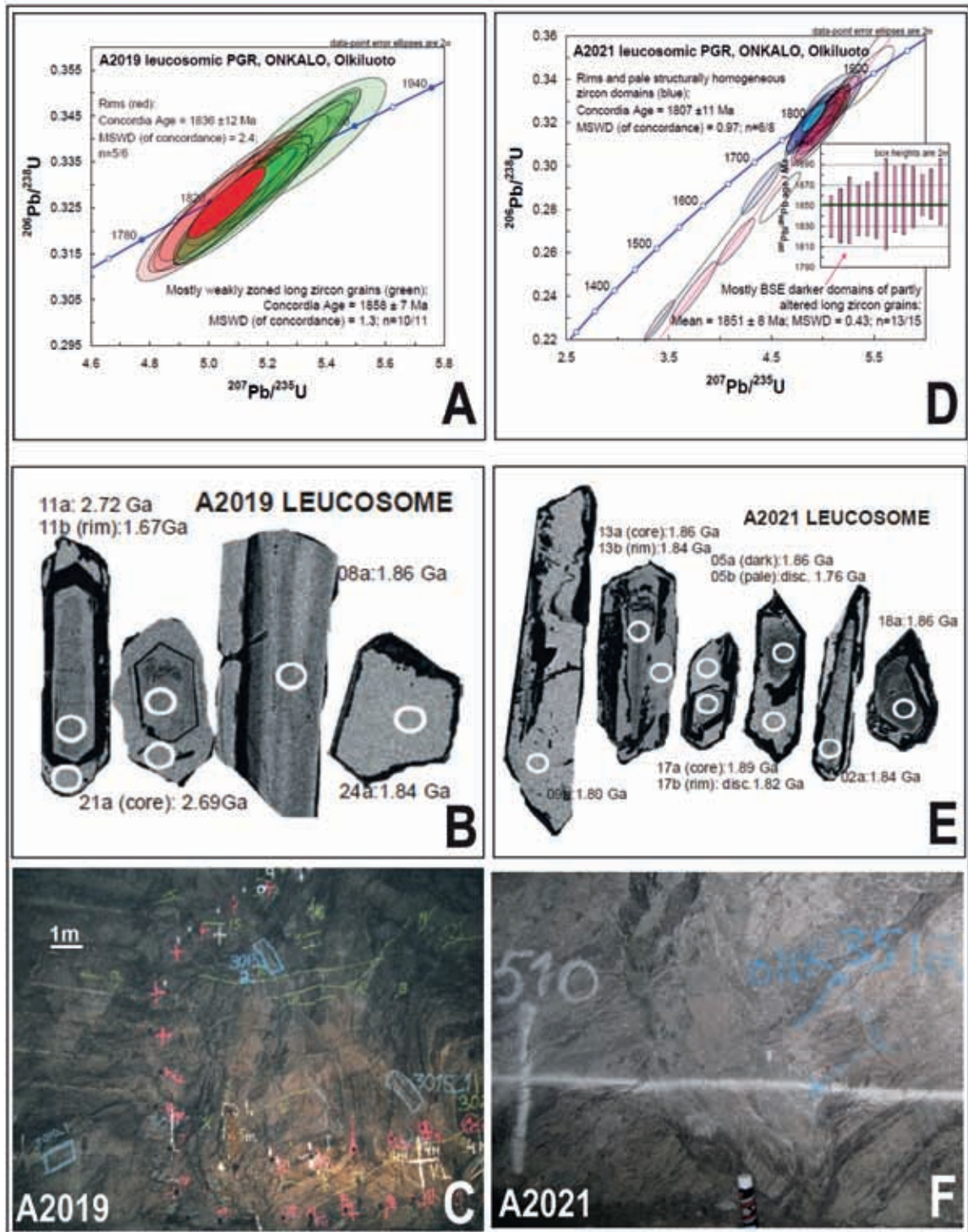


Figure 10. Concordia diagrams showing LA-MC-ICPMS zircon U-Pb isotope data for leucosomic pegmatitic samples. a) Concordia diagram for sample A2019. b) BSE-images for zircon samples A2019 with ages of core and rim. c) Sample location for the leucosomic pegmatitic sample A2019. d) Concordia diagram for sample A2021. e) BSE-images for zircon samples A2021 with ages of core and rim. f) Sample location for the leucosomic pegmatitic sample A2021. All sample sites are from the ONKALO® research tunnel situated in the middle of the Olkiluoto site, see Figure 3.

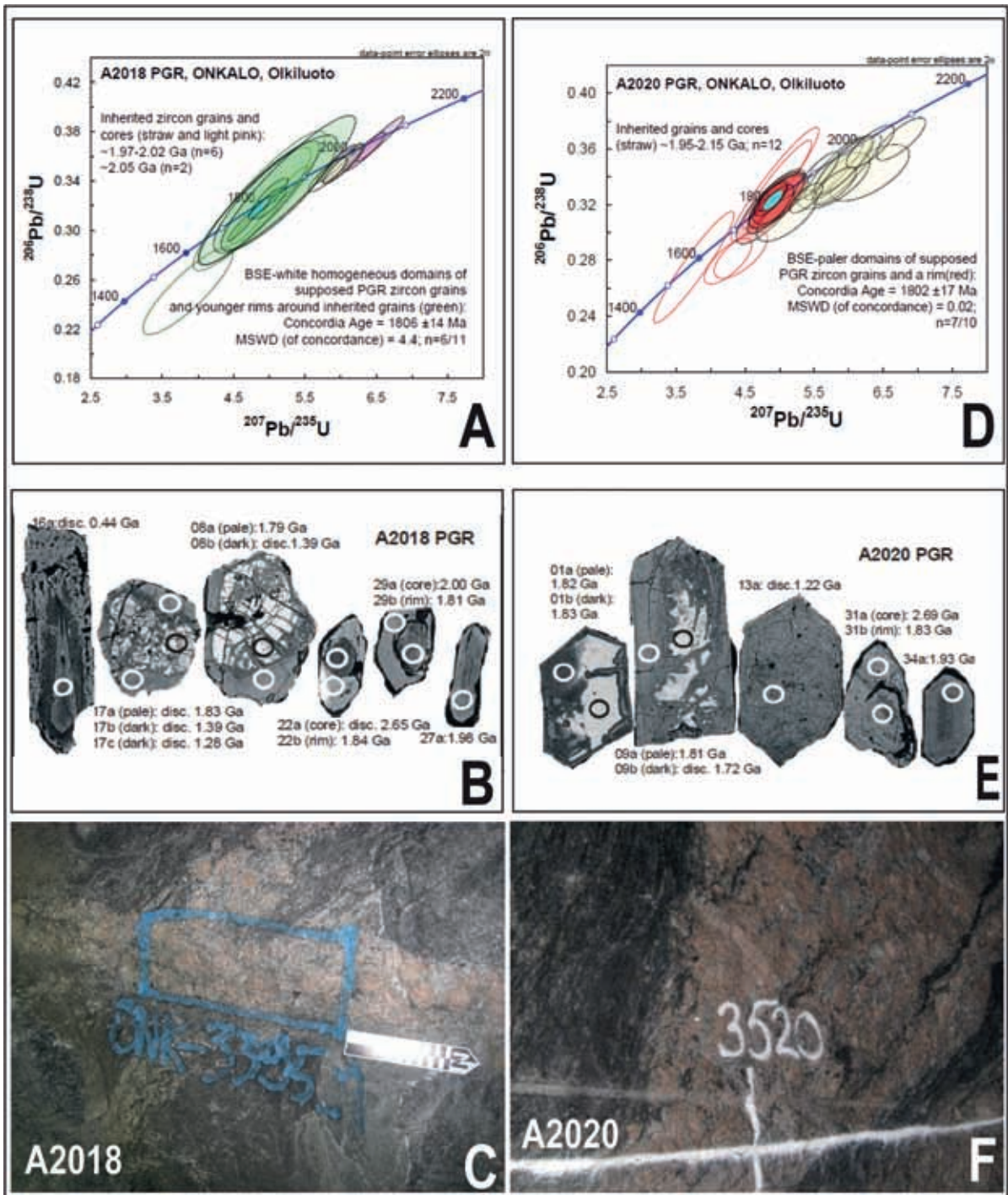


Figure 11. Concordia diagrams showing LA-MC-ICPMS zircon U-Pb isotope data for cross-cutting pegmatitic granitic samples. a) Concordia diagram for sample A2018. b) BSE-images for zircon samples A2018 with ages of core and rim. c) Sample location for the pegmatitic granitic sample A2018. d) Concordia diagram for sample A2020. e) BSE-images for zircon samples A2020 with ages of core and rim. f) Sample location for the pegmatitic granitic sample A2020. All sample sites are from the ONKALO® research tunnel situated in the middle of the Olkiluoto site, see Figure 3.

The samples A2018 and A2020 were picked out from pegmatitic veins/dykes that clearly were crosscutting the older migmatitic rock, thus indicating later phases of deformation. These yielded partly overlapping zircon concordia ages of 1806 ± 14 Ma (A2018) and 1802 ± 17 Ma (A2020) (Fig. 11). The metamorphic zircon rims and domains indicate multiphase overprinting ranging from ca. 1.82 Ga to 1.78 Ga, thus reflecting younger ages than the migmatite. The zircon grain rims and their concordia age is interpreted to reflect the second metamorphic phase and thus the second migmatite event (Fig. 11). The weakly zoned grains are defined to reflect some overgrowth from later phases of deformation.

The high-U zircons of the granitic pegmatitic veins/dykes also suffered major lead loss during the Rapakivi intrusion at ca. 1.58 Ga, and finally, a few grains yielded early Devonian ages of ca. 400 Ma (Electronic Appendix A). These can be observed as lower intercepts of the concordia in especially sample A2021.

6. Interpretation of structures and tectonic evolution at Olkiluoto

The ductile deformation (D_1 – D_4) at the Olkiluoto site can be defined with “counter-clockwise” strain rotation starting from a roughly N–S direction and ending in an E–W direction (Fig. 12). The D_1 structures are often obliterated and overprinted by subsequent deformation phases, but especially in TGG protolithic migmatites in the NW part of Olkiluoto, a few F_1 fold structures can be observed and leucosomes from the first migmatization event are present. More evident D_1 deformation is the stretching lineation L_1 , which is present in the more rigid TGG bodies. The structures of the first deformation phase indicate the inferred contractional strain direction at that stage to be orientated approximately SSW–NNE, where the orogen-parallel stretching L_1 lineation is interpreted

as concurrent with the main thrusting event of the Svecofennian orogeny. The first main migmatite producing event (M_1) is also deduced to this same stage of deformation (Fig. 12). Thus, this first deformation phase plausibly has had a significant impact in SW Finland, even though the structural remnants in Olkiluoto are limited.

After the main thrusting event (D_1/M_1), it seems that there was a stage of tectonic quiescence in Olkiluoto, although an extensional stage might have been active elsewhere in S Finland. The next stage of contractional deformation in Olkiluoto is inferred by a N–S strain direction, where earlier migmatites were pervasively deformed by the D_2 deformation, as demonstrated by isoclinal F_2 folding. During this stage, the more rigid TGG bodies were also deformed, resulting in boudinage structures. The TGG bodies show a lineation towards plunging gently to the E, which coincides with the shallowly plunging F_2 fold axis in the migmatitic, more heterogeneous rocks (Fig. 12).

The high-T tectonic-metamorphic evolution continued in the third deformation phase. This deformation phase shows overturned F_3 fold structures and E–W-striking shear zones where the deformation is distributed asymmetrically within the bedrock (Fig. 12). Due to enhanced melt transport and increased deformation, strain pockets and voids opened where pull-apart-type granitic to pegmatitic dykes/veins intruded into the migmatite. The D_3 deformation is defined as a separate deformation stage but is closely associated with the D_2 deformation phase. F_3 folding is mostly considered as rotational F_2 folds, while the E–W shearing used conduits of earlier D_2 deformation. The NW–SE-orientated strain yielded D_3 deformation with thrusting from the SE accompanied by shearing along the limbs of F_3 folds, together with oblique dextral strike-slip shearing along the E–W-orientated zones (Fig. 12). The D_3 deformation is composed of wider shear zone networks with small-scale folds and interconnected step-over shear zones, with a NE–SW orientation on the limbs of these folds. These ductile shear zones typically have brittle faulting connected and

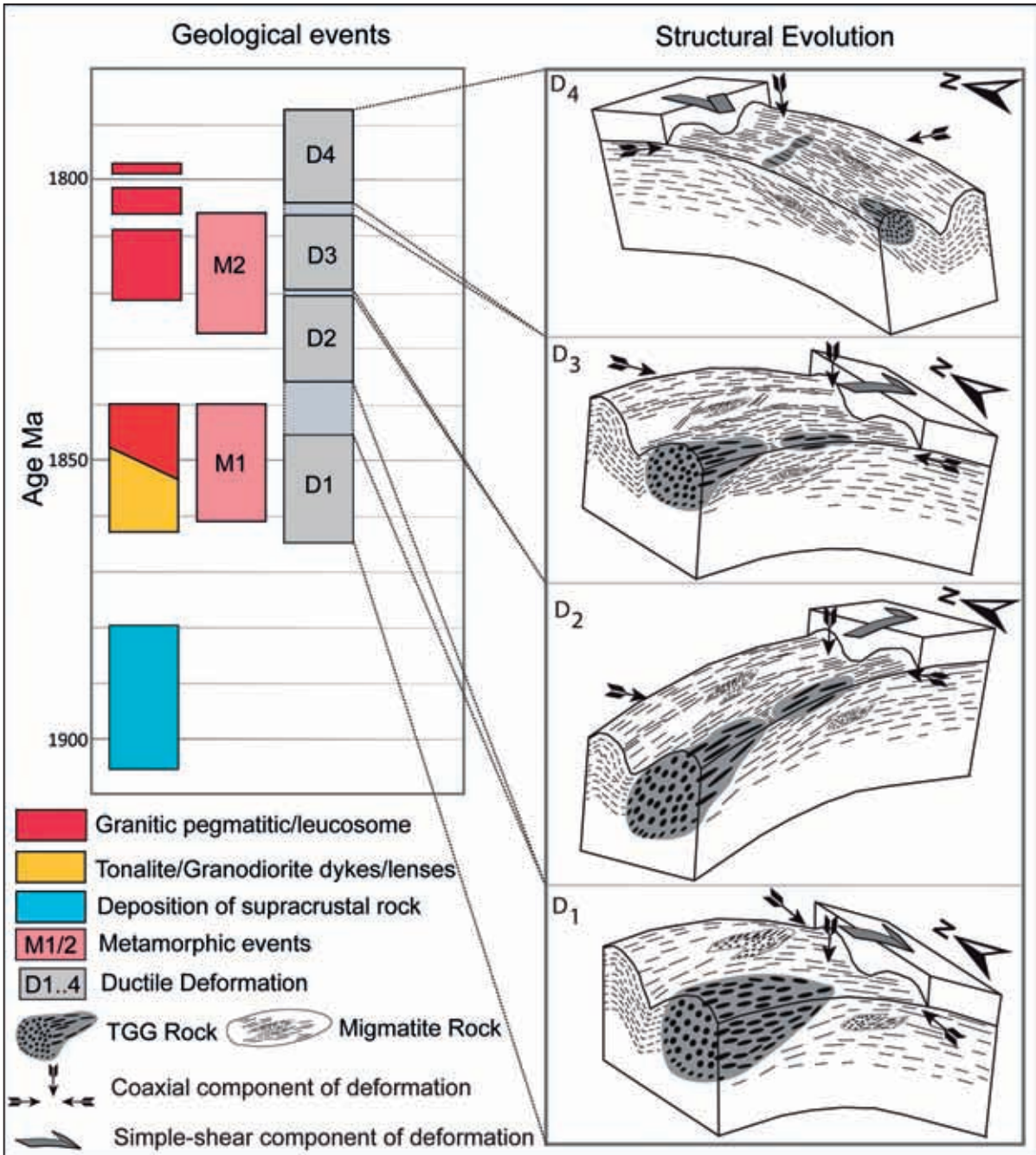


Figure 12. Diagram summarizing the structural evolution, metamorphic events, and the succession of the ductile deformation phases of the Olkiluoto area.

parallel to the ductile deformation. Another feature for the E–W-striking D_3 shear zones, especially in the northern part of Olkiluoto island, is that they accommodate shear-induced sillimanite. This can be interpreted to be formed parallel to existing foliation planes due to strain partitioning within these zones, similarly as described by Musumeci (2002).

D_4 structural features are present in the whole site but are mainly concentrated in the eastern part of Olkiluoto island (Fig. 3). The D_4 deformation is characterized by upright, gentle to tight folds, with axial surfaces trending NNE–SSW, occasionally associated with shear structures on the limbs of F_4 folds (Fig. 12). The axial planes strike NNE–SSW and dip towards the E, with a steep to moderate dip in the surface section, whereas the dip at depth is shallower. D_4 is also comprised of wider (0.1–2 m) shear zones, composed of a certain type of diatexitic migmatite with roundish quartz-feldspar megacrysts, which overprint the older structures. This rock type infers the lowest grade and metamorphic conditions for the last ductile deformation phase.

The products of the first deformation phase (D_1) are related to an older metamorphic event, M1, with a pressure of ca. 6 kbar (Tuisku & Kärki, 2010). The protolith related to this deformation phase implies an age between 1.87–1.84 Ga (Fig. 12), which is interpreted to be contemporary with or slightly younger than the main thrusting events of the Svecofennian orogeny in Southern Finland. The second metamorphic event, M2, is inferred from cross-cutting pegmatitic granitic leucosome dykes, occurring parallel to larger F_3 folds in the central part of Olkiluoto, yielding an age from 1.82 Ga to 1.78 Ga (Fig. 12). The determined pressure and temperature conditions of the second metamorphic event are 660–700 °C and 3.7–4.2 kbar (Tuisku & Kärki, 2010). Since the third deformation event produced new cross-cutting pegmatitic leucosomes, it is inferred that this amphibolite facies metamorphic event is at least contemporary with the D_3 deformation phase but might continue to the D_4 deformation phase (Fig. 12).

The anatectic melt has been a significant element in the tectonic evolution. Thus, the deformation of the whole system has been strongly controlled by the metamorphic conditions. The geological structures and deformation products can be related to the crustal depth of the deformation but can also be due to the rheological properties of the migmatite, depending on whether fluids were present during the deformation. The structural features and several leucosome-producing events in the Olkiluoto rocks can imply a high-grade metamorphic environment that persisted for a substantial time during the Palaeoproterozoic geological evolution (Fig. 12).

7. Discussion

Since the pioneering work of Mehnert, (1968), structural analysis of migmatites has shown the relationship between deformation and melt migration (Solar et al., 1998; Sawyer et al., 1999; Weinberg, 1999; Rosenberg, 2001; Vanderhaeghe, 2001). Edelman, (1973) described the geometric relationships between melt bodies and fold structures in migmatitic terrain in southern Finland. Thus, the relationship between migmatite formation and the ductile deformational history has been investigated in many studies in several Precambrian cratons, but our study provides new insights into the prolonged history of ductile deformation coupled with several events of migmatite formation. Bell & Hayward, (1991) concluded that if metamorphism begins very early in the deformation history, which seems to have been the case in Olkiluoto, it is probably related to the heat generated by the intrusion of granitoids. Even though the D_1 – D_4 deformation phases can be distinguished at the Olkiluoto site, in a more regional context they may have been related to the same tectonic stress field. The deviating directions of structural elements and the prolonged deformation at the Olkiluoto site can be explained by deviated strain due to a “counter-clockwise” rotation of the dominating compressional direction.

The ductile deformation and the tectonic evolution at Olkiluoto during the Svecofennian orogeny is delineated by several deformation phases in a high-grade migmatitic environment during an approximate time span of 90 Ma between 1.87–1.78 Ga, with two main migmatite-producing events. Recent studies by Tuisku & Kärki (2010) and Saukko et al. (2020) indicate two different metamorphic events at the Olkiluoto site and in adjacent areas (Vehkamäki et al., 2021). Thus, the area has experienced a long anatexis, producing melt at several times with multiple stages of leucosome production. Field observations and drill-core studies support the view that there are two groups of leucosomes: white and coarse-grained granitic and grey and fine-grained tonalitic, where the cross-cutting relationship indicates that tonalitic leucosomes are older (Engström, 2005; Saukko et al., 2020). This indicates that the tectonic evolution was hot for a long time and migmatites were produced and deformed several times during the ductile deformation history.

This evidence of a prolonged deformation with several crustal-scale melt pulses indicates that the site is similar to other areas within collisional orogens (Brown, 2007; Vanderhaeghe, 2009). A similar interpretation has been deduced further south, where the structures and the anatectic melt are strongly coupled to each other and the role of shear zones was significant during the tectonic evolution (Torvela & Kurhila, 2020). Another possible tectonic evolution is an accretionary orogenic model along the Fennoscandian active continental margin during the entire 1.9–1.8 Ga time interval. This could be coupled to tectonic switching with alternating extensional and transpressional episodes following the model of (Collins, 2002). This tectonic evolution is deduced for the Bergslagen lithotectonic unit and Ljusdal lithotectonic unit in Sweden (Hermansson et al., 2008; Högdahl & Bergman, 2020; Stephens, 2020a). Nonetheless, the tectonic evolution, the first deformation phase is interpreted to be related to a main thrusting event phase during the Svecofennian orogeny, and the mechanism can

be attributed to deformation in a constrictional thrusting environment, as described by Sullivan (2013). These few L-tectonite TGG bodies within the more heterogeneous and folded migmatites are the clearest evidence for strain partition within contrasting rheology, during D_1 deformation (Fig. 12). Thus, the few TGG bodies with $L>S$ observed indicate a comparable structural evolution to that seen in the Boy Scout Camp Granodiorite within the Laramie Mountains of Wyoming (Sullivan, 2006). Anatectic melt within the middle crust is only one factor that may control the localization of deformation and development of structures. Other important factors are inherited or developing structures, overall crustal fabric (an)isotropy and lithological changes (Lee et al., 2018; Torvela and Kurhila, 2020). This is demonstrated at the Olkiluoto site, where the E–W-orientated shear zones and the TGG rocks show contrasting and different deformation styles compared to the folded migmatites, which comprise the dominant rock type at the site. Füsseis et al. (2006) described an analogous environment for the development of shear zone networks in the Cap de Creus area, NE Spain.

The Olkiluoto area differs from the metamorphic evolution in S Finland since the latter metamorphic event in this area shows granulite facies metamorphism compared to our study that infers amphibolite facies (Väisänen & Hölträ, 1999; Väisänen et al., 2002). However, Högdahl et al. (2012) have shown that the Ljusdal lithotectonic unit (Fig. 1&2) in central E Sweden has two different metamorphic peaks, characterized by low-P and high- or medium-T conditions, defined by shallow to moderately dipping shear zones emplacing older, granulite-facies rocks on top of younger amphibolite-facies rocks. The mineral assemblage in the Ljusdal lithotectonic unit is defined by cordierite–sillimanite–garnet in the migmatites (Högdahl & Bergman, 2020). The similar mineral assemblage in the Olkiluoto migmatites points to a similar metamorphic environment for the Olkiluoto site. Högdahl et al. (2012) also deduced that (1) thrusting was indeed

an important component during the tectonic evolution and (2) the Svecofennian is not only a hot, but also a slow cooling orogen.

Since the Bothnian sea hinders direct geological correlations between the land areas of Finland and Sweden, other means of investigation are essential. Crustal-scale features have been interpreted from BABEL profiles as collisional structures defining a N-dipping Palaeoproterozoic subduction zone (Fig. 2) during the main thrusting phase of the Svecofennian orogeny (1.89–1.87 Ga) (BABEL Working Group, 1993; Korja & Heikkinen, 2005). The seismic interpretations also infer an extensional event between this first main crustal shortening event and the next accretionary stage (1.84–1.81 Ga) (Högdahl & Bergman, 2020; Korja & Heikkinen, 2005). This event would have increased the average crustal temperatures, and thus acted as the main heat source for the later collisional low-*P*/high-*T* metamorphism. Korja & Heikkinen (2005) defined that the second crustal shortening event (accretionary stage 1.84–1.81 Ga) caused stacking due to thrusting of hot extended crustal slices that formed new granites and migmatites in SW Finland and Central E Sweden. This second phase of metamorphism at the Olkiluoto site is associated with new granite and leucosome formation during the later phases of deformation, D_3 – D_4 . Thus, the Olkiluoto site is one of the few locations in S Finland where long-lasting tectonic evolution and multiple metamorphic events have been interpreted and defined.

8. Conclusions

Our research has revealed that the rocks in Olkiluoto underwent four different ductile deformation phases during the Palaeoproterozoic Svecofennian orogeny. This study also demonstrated that the tectonic evolution was comprised of at least two metamorphic events producing migmatite rocks during a period of approximately 90 Ma. The structural data and the age determinations provided in this paper, together

with the metamorphic data presented in Tuisku & Kärki (2010), suggest that the Olkiluoto area and the Ljusdal lithotectonic unit show remarkable similarities of the deformation history. The older, granulite-facies metamorphism with later, younger amphibolite-facies metamorphism in the Ljusdal lithotectonic unit is in accordance with the two metamorphic peaks in Olkiluoto, where the older one is hotter and the younger one is an amphibolite-facies metamorphism with roughly the same age as in Ljusdal. Thus, the new data presented in this paper supports the proposed connection between rocks in SW Finland and central eastern Sweden. If Olkiluoto can be considered as part of the Ljusdal lithotectonic unit, the major Kynsikangas shear zone, located 40 km NE of Olkiluoto, might be a major block boundary between the lithotectonic units, as suggested by Gaál & Gorbatshev (1987) and Torvela & Ehlers (2010).

The impacts of ductile deformation processes in high-grade migmatitic rocks of Olkiluoto vary in different subareas of the study area. Thus, it is possible to outline units where the products of a particular deformation phase or a combination of phases dominate, but, on the other hand, some features of all four deformations have been recognized all over the area. The structural geological evolution at Olkiluoto provides some new insights into the tectonic history of SW Finland and the main outcomes of the study are as follows:

- The Olkiluoto site displays a high-grade migmatitic environment with two main migmatite-producing events during a time span of approximately 90 Ma between 1.87–1.78 Ga.
- The bedrock has been subjected to ductile deformation in four different phases, evidenced by multiple folding phases, various ductile shear events recognised through cross-cutting features and distinct types of deformation.
- The L_1 stretching lineation direction and F_1 folding are indications of the first crustal shortening event and accompanied thrusting due to the Svecofennian orogeny.

- The D_2 – D_4 deformation phases are associated with a second accretionary stage together with a second phase of metamorphism during the next stages of the Svecofennian orogeny.
- The interpreted metamorphic and tectonic evolution suggests long-lasting, high-grade migmatite development and a slow-cooling orogenic history.
- The newly acquired data point to a structural history and tectonic evolution similar to the Ljusdal lithotectonic unit in Central E Sweden, thus providing new evidence for coupling of the Palaeoproterozoic bedrock of Sweden and Finland.

Acknowledgements

M. Karhunen, L. Järvinen, T. Hokkanen, A. Pulkkinen, L. Heikkinen, and M. Tiljander are thanked for rock crushing, mineral separation, sample preparation, TIMS mass spectrometry, mount preparation, and XRD-identification of dumortierite, respectively. The authors also wish to give a special thanks to K. Högdahl and A-K. Korja for their constructive comments on the early versions of the manuscript. The reviews by the Editor-in-Chief, Associate Editor A. Luttinen and the officially appointed Journal Reviewers S. Grigull and A. Rotevatn all helped to improve the final version of the manuscript. We are grateful to Posiva Oy for the support during the field work, and access to the data.

Supplementary data

Electronic Appendices are available via Bulletin of the Geological Society Finland web page.

Electronic Appendix A: Data table for U-Pb samples A2018, A2019 A2020 and A2021.

References

- Andersen, T., Griffin, W.L., Jackson, S.E., Knudsen, T.-L., Pearson, N.J., 2004. Mid-Proterozoic magmatic arc evolution at the southwest margin of the Baltic Shield. *Lithos* 73, 289–318.
<https://doi.org/10.1016/j.lithos.2003.12.011>
- BABEL Working Group, 1993. Integrated Seismic Studies of the Baltic Shield Using Data In the Gulf of Bothnia Region. *Geophysical Journal International* 112, 305–324.
<https://doi.org/10.1111/j.1365-246X.1993.tb01172.x>
- Bell, T.H., Hayward, N., 1991. Episodic metamorphic reactions during orogenesis: the control of deformation partitioning on reaction sites and reaction duration. *Journal of Metamorphic Geology* 9, 619–640.
<https://doi.org/10.1111/j.1525-1314.1991.tb00552.x>
- Belousova, E.A., Griffin, W.L., O'reilly, S.Y., 2006. Zircon Crystal Morphology, Trace Element Signatures and Hf Isotope Composition as a Tool for Petrogenetic Modelling: Examples From Eastern Australian Granitoids. *Journal of Petrology* 47, 329–353.
<https://doi.org/10.1093/petrology/egi077>
- Bergman, S., Högdahl, K., Nironen, M., Ogenhall, E., Sjöström, H., Lundqvist, L., Lahtinen, R., 2008. Timing of Palaeoproterozoic intra-orogenic sedimentation in the central Fennoscandian Shield; evidence from detrital zircon in metasandstone. *Precambrian Research* 161, 231–249.
<https://doi.org/10.1016/j.precamres.2007.08.007>
- Brown, M., 2007. Crustal melting and melt extraction, ascent and emplacement in orogens: mechanisms and consequences. *Journal of the Geological Society* 164, 709–730.
<https://doi.org/10.1144/0016-76492006-171>
- Brown, M., Solar, G.S., 1998a. Shear-zone systems and melts: feedback relations and self-organization in orogenic belts. *Journal of Structural Geology* 20, 211–227.
[https://doi.org/10.1016/S0191-8141\(97\)00068-0](https://doi.org/10.1016/S0191-8141(97)00068-0)
- Brown, M., Solar, G.S., 1998b. Granite ascent and emplacement during contractional deformation in convergent orogens. *Journal of Structural Geology* 20, 1365–1393.
[https://doi.org/10.1016/S0191-8141\(98\)00074-1](https://doi.org/10.1016/S0191-8141(98)00074-1)
- Buntin, S., Malehmir, A., Koyi, H., Högdahl, K., Malinowski, M., Larsson, S.Å., Thybo, H., Juhlin, C., Korja, A., Górszczyk, A., 2019. Emplacement and 3D geometry of crustal-scale saucer-shaped intrusions in the Fennoscandian Shield. *Nature Scientific Reports*, Volume 9, Issue 1.
<https://doi.org/10.1038/s41598-019-46837-x>
- Castro, A., Fernández, C., El-Hmidi, H., El-Biad, M., Díaz, M., de la Rosa, J., Stuart, F., 1999. Age constraints to the relationships between magmatism, metamorphism and tectonism in the Aracena metamorphic belt, southern Spain. *International Journal of Earth Sciences* 88, 26–37.
<https://doi.org/10.1007/s005310050243>

- Chopin, F., Korja, A., Nikkilä, K., Hölttä, P., Korja, T., Zaher, M.A., Kurhila, M., Eklund, O., Rämö, O.T., 2020. The Vaasa Migmatitic Complex (Svecofennian Orogen, Finland): Buildup of a LP-HT Dome During Nuna Assembly. *Tectonics* 39. <https://doi.org/10.1029/2019TC005583>
- Collins, W.J., 2002. Hot orogens, tectonic switching, and creation of continental crust. *Geology* 30, 535–538. [https://doi.org/10.1130/0091-7613\(2002\)030<0535:HOTSAC>2.0.CO;2](https://doi.org/10.1130/0091-7613(2002)030<0535:HOTSAC>2.0.CO;2)
- Edelman, N., 1973. Tension cracks parallel with the axial plane. *Bulletin Geological Society of Finland* 45, 61–65. <https://doi.org/10.17741/bgsf/45.1.009>
- Engström, J., 2005. Geological mapping of investigation trench OL-TK8 at the Olkiluoto study site, Eurajoki, SW Finland. (Working Report No. 2005–44), Posiva Working Report. Posiva Oy, Eurajoki.
- Fussey, F., Handy, M.R., Schrank, C., 2006. Networking of shear zones at the brittle-to-viscous transition (Cap de Creus, NE Spain). *Journal of Structural Geology* 28, 1228–1243. <https://doi.org/10.1016/j.jsg.2006.03.022>
- Gaál, G., Gorbatshev, R., 1987. An Outline of the Precambrian Evolution of the Baltic Shield. *Precambrian Research* 17, 149–159. [https://doi.org/10.1016/0301-9268\(87\)90044-1](https://doi.org/10.1016/0301-9268(87)90044-1)
- Hegner, E., Chen, F., Hann, H.P., 2001. Chronology of basin closure and thrusting in the internal zone of the Variscan belt in the Schwarzwald, Germany: evidence from zircon ages, trace element geochemistry, and Nd isotopic data. *Tectonophysics* 332, 169–184. [https://doi.org/10.1016/S0040-1951\(00\)00254-7](https://doi.org/10.1016/S0040-1951(00)00254-7)
- Hermansson, T., Stephens, M.B., Corfu, F., Page, L.M., Andersson, J., 2008. Migratory tectonic switching, western Svecofennian orogen, central Sweden: Constraints from U/Pb zircon and titanite geochronology. *Precambrian Research* 161, 250–278. <https://doi.org/10.1016/j.precamres.2007.08.008>
- Högdahl, K., Bergman, S., 2020. Chapter 5 Paleoproterozoic (1.9–1.8 Ga), syn-orogenic magmatism and sedimentation in the Ljusdal lithotectonic unit, Svecokarelian orogen. *Geological Society, London, Memoirs* 50, 131–153. <https://doi.org/10.1144/M50-2016-30>
- Högdahl, K., Majka, J., Sjöström, H., Nilsson, K.P., Claesson, S., Konečný, P., 2012. Reactive monazite and robust zircon growth in diatexites and leucogranites from a hot, slowly cooled orogen: implications for the Palaeoproterozoic tectonic evolution of the central Fennoscandian Shield, Sweden. *Contributions to Mineralogy and Petrology* 163, 167–188. <https://doi.org/10.1007/s00410-011-0664-x>
- Högdahl, K., Sjöström, H., Andersson, U.B., Ahl, M., 2008. Continental margin magmatism and migmatization in the west-central Fennoscandian Shield. *Lithos* 102, 435–459. <https://doi.org/10.1016/j.lithos.2007.07.019>
- Horstwood, M.S.A., Foster, G.L., Parrish, R.R., Noble, S.R., Nowell, G.M., 2003. Common-Pb corrected in situ U–Pb accessory mineral geochronology by LA-MC-ICP-MS. *Journal of Analytical Atomic Spectrometry* 18, 837–846. <https://doi.org/10.1039/B304365G>
- Huhma, H., 1986. Sm–Nd, U–Pb and Pb–Pb isotopic evidence for the origin of the Early Proterozoic Svecokarelian crust in Finland. *Geological Survey of Finland, Bulletin* 337, 1–48.
- Huhma, H., Mänttari, I., Kontinen, P., Halkoaho, A., Hanski, T., Hokkanen, E., Layahe, J., Vaajoki, P., Whitehouse, M., Huhma, Hannu, Mänttari, Irmeli, Peltonen, P., Kontinen, A., Halkoaho, T., Hanski, E., Hokkanen, T., Hölttä, P., Juopperi, H., Konnunaho, J., Whitehouse, Martin, 2012. The age of the Archaean greenstone belts in Finland. *Geological Survey of Finland, Special Paper* 54, 74–174.
- Jackson, S.E., Pearson, N.J., Griffin, W.L., Belousova, E.A., 2004. The application of laser ablation-inductively coupled plasma-mass spectrometry to in situ U–Pb zircon geochronology. *Chemical Geology* 211, 47–69. <https://doi.org/10.1016/j.chemgeo.2004.06.017>
- Johannes, W., Ehlers, C., Kriegsman, L.M., Mengel, K., 2003. The link between migmatites and S-type granites in the Turku area, southern Finland. *Lithos* 68, 69–90. [https://doi.org/10.1016/S0024-4937\(03\)00032-X](https://doi.org/10.1016/S0024-4937(03)00032-X)
- Kähkönen, Y., 2005. Chapter 8 Svecofennian supracrustal rocks, in: Lehtinen, M., Nurmi, P.A., Rämö, O.T. (Eds.), *Developments in Precambrian Geology, Precambrian Geology of Finland Key to the Evolution of the Fennoscandian Shield*. Elsevier, pp. 343–405. [https://doi.org/10.1016/S0166-2635\(05\)80009-X](https://doi.org/10.1016/S0166-2635(05)80009-X)
- Kärki, A., 2015. Migmatites and Migmatite-Like Rocks of Olkiluoto (Working Report No. 2015–03), Posiva Working Report. Posiva Oy, Eurajoki.
- Kohonen, J., Lahtinen, R., Luukas, J., Nironen, M., 2021. Classification of regional-scale tectonic map units in Finland. *Geological Survey of Finland, Bulletin* 412, 33–80. <https://doi.org/10.30440/bt412.2>
- Koistinen, T., Bogatchev, V., Stephens, M.B., Nordgulen, O., Wennerström, M., Korhonen, J., 2001. Geological map of the Fennoscandian Shield scale 1:2 000 000.
- Korja, A., Heikkinen, P., Aaro, S., 2001. Crustal structure of the northern Baltic Sea palaeorift. *Tectonophysics* 331, 341–358. [https://doi.org/10.1016/S0040-1951\(00\)00290-0](https://doi.org/10.1016/S0040-1951(00)00290-0)
- Korja, A., Heikkinen, P., 2005. The accretionary Svecofennian orogen—insight from the BABEL profiles. *Precambrian Research* 136, 241–268. <https://doi.org/10.1016/j.precamres.2004.10.007>
- Korsman, K., Koistinen, T., Kohonen, J., Wennerström, M., Ekdahl, E., Honkamo, M., Idman, H., Pekkala, Y. (Eds.) 1997. Bedrock map of Finland 1:1 000 000. Geological Survey of Finland.
- Korsman, K., Korja, T., Pajunen, M., Virransalo, P., GGT/SVEKA Working Group, 1999. The GGT/SVEKA Transect: Structure and Evolution of the Continental Crust in the Paleoproterozoic Svecofennian Orogen in

- Finland. *International Geology Review* 41, 287–333.
<https://doi.org/10.1080/00206819909465144>
- Lahtinen, R., 1994. Crustal evolution of the Svecofennian and Karelian domains during 2.1 - 1.79 Ga: with special emphasis on the geochemistry and origin of 1.93 - 1.91 Ga gneissic tonalites and associated supracrustal rocks in the Rautalampi area, central Finland. *Geological Survey of Finland, Bulletin* 378, 0-128.
- Lahtinen, R., Korja, A., Nironen, M., 2005. Chapter 11 Paleoproterozoic tectonic evolution. In: Lehtinen, M., Nurmi, P.A., Rämö, O.T. (Eds.), *Developments in Precambrian Geology, Precambrian Geology of Finland Key to the Evolution of the Fennoscandian Shield*. Elsevier, 481–531.
[https://doi.org/10.1016/S0166-2635\(05\)80012-X](https://doi.org/10.1016/S0166-2635(05)80012-X)
- Lee, A.L., Torvela, T., Lloyd, G.E., Walker, A.M., 2018. Melt organisation and strain partitioning in the lower crust. *Journal of Structural Geology* 113, 188–199.
<https://doi.org/10.1016/j.jsg.2018.05.016>
- Ludwig, K.R., 2003. *Users manual for Isoplot/Ex: a geochronological toolkit for Microsoft Excel*. Berkeley Geochronology Center Special Publication 1a, 53.
- Mäkitie, H., Sipilä, P., Kujala, H., Lindberg, A., Kotilainen, A., 2012. Formation mechanism of the Vaasa Batholith in the Fennoscandian shield: Petrographic and geochemical constraints. *Bulletin Geological Society of Finland* 84, 141–166.
<https://doi.org/10.17741/bgsf/84.2.003>
- Mänttari, I., Talikka, M., Paulamäki, S., Mattila, J., 2006. U-Pb ages for tonalitic gneiss, pegmatitic granite, and diabase dyke, Olkiluoto study site, Eurajoki, SW Finland (Working Report No. 2006–12), Posiva Working Report. Posiva Oy, Eurajoki.
- Mänttari, I., Aaltonen, I., Lindberg, A., 2007. U-Pb Ages for Two Tonalitic Gneisses, Pegmatitic Granites, and K-feldspar Porphyries, Olkiluoto Study Site, Eurajoki, SW Finland (Working Report No. 2007–70), Posiva Working Report. Posiva Oy, Eurajoki.
- Mehnert, K.R., 1968. Migmatites and the origin of granitic rocks. *Megascopic Struct. Migmatite* 7–42.
- Milord, I., 2001. Formation of Diatexite Migmatite and Granite Magma during Anatexis of Semi-pelitic Metasedimentary Rocks: an Example from St. Malo, France. *Journal of Petrology* 42, 487–505.
<https://doi.org/10.1093/petrology/42.3.487>
- Musumeci, G., 2002. Sillimanite-bearing shear zones in syntectonic leucogranite: fluid-assisted brittle–ductile deformation under amphibolite facies conditions. *Journal of Structural Geology* 24, 1491–1505.
[https://doi.org/10.1016/S0191-8141\(01\)00153-5](https://doi.org/10.1016/S0191-8141(01)00153-5)
- Nironen, M., 2017. Bedrock of Finland at the scale 1:1 000 000 – Major stratigraphic units, metamorphism and tectonic evolution, Geological Survey of Finland, Special Paper 60.
- Nironen, M., 2005. Chapter 10 Proterozoic orogenic granitoid rocks, in: Lehtinen, M., Nurmi, P.A., Rämö, O.T. (Eds.), *Developments in Precambrian Geology, Precambrian Geology of Finland Key to the Evolution of the Fennoscandian Shield*. Elsevier, pp. 443–479.
[https://doi.org/10.1016/S0166-2635\(05\)80011-8](https://doi.org/10.1016/S0166-2635(05)80011-8)
- Rosa, D.R.N., Finch, A.A., Andersen, T., Inverno, C.M.C., 2009. U–Pb geochronology and Hf isotope ratios of magmatic zircons from the Iberian Pyrite Belt. *Mineralogy and Petrology* 95, 47–69.
<https://doi.org/10.1007/s00710-008-0022-5>
- Rosenberg, C.L., 2001. Deformation of partially molten granite: a review and comparison of experimental and natural case studies. *International Journal of Earth Sciences* 90, 60–76.
<https://doi.org/10.1007/s005310000164>
- Saukko, A., Ahläng, C., Nikkilä, K., Soesoo, A., Eklund, O., 2020. Double Power-Law in Leucosome Width Distribution: Implications for Recognizing Melt Movement in Migmatites. *Frontiers in Earth Science* 8.
<https://doi.org/10.3389/feart.2020.591871>
- Sawyer, E.W., 1998. Formation and Evolution of Granite Magmas During Crustal Reworking: the Significance of Diatexites. *Journal of Petrology* 39, 1147–1167.
<https://doi.org/10.1093/etroj/39.6.1147>
- Sawyer, E.W., Dombrowski, C., Collins, W.J., 1999. Movement of melt during synchronous regional deformation and granulite-facies anatexis, an example from the Wuluma Hills, central Australia. *Geological Society, London, Special Publications* 168, 221–237.
<https://doi.org/10.1144/GSL.SP.1999.168.01.15>
- Skyttä, P., Mänttari, I., 2008. Structural setting of late Svecofennian granites and pegmatites in Uusimaa Belt, SW Finland: Age constraints and implications for crustal evolution. *Precambrian Research* 164, 86–109.
<https://doi.org/10.1016/j.precamres.2008.04.001>
- Solar, G.S., Brown, M., 2001. Petrogenesis of Migmatites in Maine, USA: Possible Source of Peraluminous Leucogranite in Plutons? *Journal of Petrology* 42, 789–823.
<https://doi.org/10.1093/petrology/42.4.789>
- Solar, G.S., Pressley, R.A., Brown, M., Tucker, R.D., 1998. Granite ascent in convergent orogenic belts: Testing a model. *Geology* 26, 711.
[https://doi.org/10.1130/0091-7613\(1998\)026<0711:GAICOB>2.3.CO;2](https://doi.org/10.1130/0091-7613(1998)026<0711:GAICOB>2.3.CO;2)
- Stacey, J.S., Kramers, J.D., 1975. Approximation of terrestrial lead isotope evolution by a two-stage model. *Earth and Planetary Science Letters* 26, 207–221.
[https://doi.org/10.1016/0012-821X\(75\)90088-6](https://doi.org/10.1016/0012-821X(75)90088-6)
- Stephens, M.B., 2020a. Chapter 8 Outboard-migrating accretionary orogeny at 1.9–1.8 Ga (Svecokarelian) along a margin to the continent Fennoscandia. *Geological Society, London, Memoirs* 50, 237–250.
<https://doi.org/10.1144/M50-2019-18>
- Stephens, M.B., 2020b. Chapter 1 Introduction to the lithotectonic framework of Sweden and organization of this Memoir. *Geological Society, London, Memoirs* 50, 1–15.
<https://doi.org/10.1144/M50-2019-21>

- Stephens, M.B., Andersson, J., 2015. Migmatization related to mafic underplating and intra- or back-arc spreading above a subduction boundary in a 2.0–1.8Ga accretionary orogen, Sweden. *Precambrian Research* 264, 235–257.
<https://doi.org/10.1016/j.precamres.2015.04.019>
- Sullivan, W.A., 2006. Structural Significance of L Tectonites in the Eastern-Central Laramie Mountains, Wyoming. *The Journal of Geology* 114, 513–531.
<https://doi.org/10.1086/506158>
- Sullivan, W.A., 2013. L tectonites. *Journal of Structural Geology*, Deformation localization in rocks 50, 161–175.
<https://doi.org/10.1016/j.jsg.2012.01.022>
- Torvela, T., Mänttari, I., Hermansson, T., 2008. Timing of deformation phases within the South Finland shear zone, SW Finland. *Precambrian Research* 160, 277–298.
<https://doi.org/10.1016/j.precamres.2007.08.002>
- Torvela, T., Ehlers, C., 2010. Microstructures associated with the Sottunga-Jurmo shear zone and their implications for the 1.83–1.79 Ga tectonic development of SW Finland. *Bulletin Geological Society of Finland* 82, 5–29.
<https://doi.org/10.17741/bgsf/82.1.001>
- Torvela, T., Kurhila, M., 2020. How does orogenic crust deform? Evidence of crustal-scale competent behaviour within the partially molten middle crust during orogenic compression. *Precambrian Research* 342, 105670.
<https://doi.org/10.1016/j.precamres.2020.105670>
- Tuisku, P., Kärki, A., 2010. Metamorphic Petrology of Olkiluoto (Working Report No. 2010–54), Posiva Working Report. Posiva Oy, Eurajoki.
- Väisänen, M., Hölttä, P., 1999. Structural and metamorphic evolution of the Turku migmatite complex, southwestern Finland. *Bulletin Geological Society of Finland* 71, 177–218.
<https://doi.org/10.17741/bgsf/71.1.009>
- Väisänen, M., Mänttari, I., Hölttä, P., 2002. Svecofennian magmatic and metamorphic evolution in southwestern Finland as revealed by U-Pb zircon SIMS geochronology. *Precambrian Research* 116, 111–127.
[https://doi.org/10.1016/S0301-9268\(02\)00019-0](https://doi.org/10.1016/S0301-9268(02)00019-0)
- Väisänen, M., Skyttä, P., 2007. Late Svecofennian shear zones in southwestern Finland. *Geologiska Föreningen i Stockholms Förhandlingar* 129, 55–64.
<https://doi.org/10.1080/11035890701291055>
- Väisänen, M., Eklund, O., Lahaye, Y., O'Brien, H., Fröjdö, S., Högdahl, K., Lammi, M., 2012. Intra-orogenic Svecofennian magmatism in SW Finland constrained by LA-MC-ICP-MS zircon dating and geochemistry. *Geologiska Föreningen i Stockholms Förhandlingar* 134, 99–114.
<https://doi.org/10.1080/11035897.2012.680606>
- Vanderhaeghe, O., 2001. Melt segregation, pervasive melt migration and magma mobility in the continental crust: the structural record from pores to orogens. *Physics and Chemistry of the Earth, Part A: Solid Earth and Geodesy* 26, 213–223.
[https://doi.org/10.1016/S1464-1895\(01\)00048-5](https://doi.org/10.1016/S1464-1895(01)00048-5)
- Vanderhaeghe, O., 2009. Migmatites, granites and orogeny: Flow modes of partially-molten rocks and magmas associated with melt/solid segregation in orogenic belts. *Tectonophysics*, Hot orogens 477, 119–134.
<https://doi.org/10.1016/j.tecto.2009.06.021>
- Vehkamäki, T., Väisänen, M., Kurhila, M., O'Brien, H., Hölttä, P., Syrjänen, J.-K., 2021. Metamorphic zones in SW Finland: monazite and zircon U-Pb dating of leucosomes in paragneisses. In: Kukkonen, I., Veikkolainen, T., Heinonen, S., Karell, F., Kozlovskaya, E., Luttinen, A., Nikkilä, K., Nykänen, V., Poutanen, M., Skyttä, P., Tanskanen, E., & Tiira, T. (Eds.) (2021). *Lithosphere 2021: Eleventh symposium on structure, composition and evolution of the lithosphere*. (Report S; Vol. 71). Institute of Seismology, University of Helsinki.
- Weinberg, R.F., 1999. Mesoscale pervasive felsic magma migration: alternatives to dyking. *Lithos* 46, 393–410.
[https://doi.org/10.1016/S0024-4937\(98\)00075-9](https://doi.org/10.1016/S0024-4937(98)00075-9)
- Wickström, L.M., Stephens, M.B., 2020. Chapter 18 Tonian–Cryogenian rifting and Cambrian–Early Devonian platform to foreland basin development outside the Caledonide orogen. *Geological Society, London, Memoirs* 50, 451–477.
<https://doi.org/10.1144/M50-2016-31>